J Electr Eng Technol.2018; 13(3): 1079-1088
http://doi.org/10.5370/JEET.2018.13.3.1079

ISSN(Print) 1975-0102
ISSN(Online) 2093-7423

# Research on Line Overload Emergency Control Strategy Based on the Source-Load Synergy Coefficient

**Jing Ma†, Wenbo Kang* and James S. Thorp****

**Abstract** – A line overload emergency control strategy based on the source-load synergy coefficient is proposed in this paper. First, the definition of the source-load synergy coefficient is introduced. When line overload is detected, the source-load branch synergy coefficient and source-load distribution synergy coefficient are calculated according to the real-time operation mode of the system. Second, the generator tripping and load shedding control node set is determined according to the source-load branch synergy coefficient. And then, according to the line overload condition, the control quantity of each control node is determined using the Double Fitness Particle Swarm Optimization (DFPSO), with minimum system economic loss as the objective function. Thus load shedding for the overloaded line could be realized. On this basis, in order to guarantee continuous and reliable power supply, on the condition that no new line overload is caused, some of the untripped generators are selected according to the source-load distribution synergy coefficient to increase power output. Thus power supply could be restored to some of the shedded loads, and the economic loss caused by emergency control could be minimized. Simulation tests on the IEEE 10-machine 39-bus system verify the effectiveness and feasibility of the proposed strategy.

**Keywords**: Emergency control, Source-load synergy coefficient, Generator tripping and load shedding, Line overload.

## 1. Introduction

When some heavily loaded lines in the power grid become overloaded, line protection may mal-operate, which may lead to cascading tripping and even blackout, endangering the safety of the whole system [1-3]. Therefore, it is vital to take emergency control measures to eliminate the overload, prevent blackout accidents, and maintain the safe and steady operation of the system, at the least cost possible [4].

Line overload emergency control strategies can be sorted into two major categories. The first category is based on the sensitivity degree [5-6], and the second category is based on objective optimization [7-9]. Emergency control strategies based on the sensitivity degree use the sensitivity of different generators and loads to the overloaded line as its load shedding capability index, and regulate in the single or equal proportion principle according to the sensitivity. This kind of strategy is simple in computing and fast in decision making. However, it is not able to make the best of the regulatory capability of the whole system to realize load shedding in a wider range. Emergency control strategies based on traditional objective optimization take full consideration of the operation state of the whole power grid, and carry out optimization search with minimum control quantity loss as the objective function. However, the generation characteristics of different generators and the economic loss characteristics of different loads are neglected [10-11].

In view of these problems, a line overload emergency control strategy based on the source-load synergy coefficient is proposed in this paper, in which the load economic loss is considered and the grid loss is quantified. First, when line overload is detected, the source-load branch synergy coefficient and source-load distribution synergy coefficient are updated according to the real-time operation mode of the system. Second, the generator tripping and load shedding control node set is determined according to the source-load branch synergy coefficient. And then, according to the line overload condition and the control node set, optimization search of the control strategy is carried out using the Double Fitness Particle Swarm Optimization (DFPSO) [12-13], with minimum system economic loss as the objective function. On this basis, in order to guarantee continuous and reliable power supply, on the condition that no new line overload is caused, part of the untripped generators are selected according to the source-load distribution synergy coefficient to increase power output. Similarly, the DFPSO is used for optimization search of the control strategy. Thus power supply could be restored to part of the shedded loads, and the economic loss caused by emergency control could

† Corresponding Author: State Key Laboratory of Alternate Electrical Power System with Renewable Energy Sources, North China Electric Power University, China. (hdmajing@163.com)
* State Key Laboratory of Alternate Electrical Power System with Renewable Energy Sources, North China Electric Power University, China.
** Bradley Department of Electrical and Computer Engineering, Virginia Polytechnic Institute and State University, USA.
Received: May 20, 2016; Accepted: January 26, 2018



Copyright ⓒ The Korean Institute of Electrical Engineers
This is an Open-Access article distributed under the terms of the Creative Commons Attribution Non-Commercial License (http://creativecommons.org/licenses/by-nc/3.0/) which permits unrestricted non-commercial use, distribution, and reproduction in any medium, provided the original work is properly cited.

be minimized. Simulation tests on the IEEE 10-machine 39-bus system verify the correctness and effectiveness of the proposed method.

## 2. Source-load Synergy Coefficient

By equating the system to a linear network (see Fig.1), and the generators and loads in the system to node injection currents, the network node voltage equation can be gained:

$$\boldsymbol{I}_{\mathrm{N}} = \boldsymbol{Y}_{\mathrm{N}}\boldsymbol{V}_{\mathrm{N}} \tag{1}$$

where $\boldsymbol{I}_{\mathrm{N}}$ is the node injection current phasor, the positive direction of which being toward the network. Therefore, the injection current of generator node is positive and the injection current of load node is negative. $\boldsymbol{V}_{\mathrm{N}}$ is the node voltage phasor and $\boldsymbol{Y}_{\mathrm{N}}$ is the node admittance matrix which can be calculated with the branch admittance matrix $\boldsymbol{Y}$ and the network node incidence matrix $\boldsymbol{A}$, i.e. $\boldsymbol{Y}_{\mathrm{N}} = \boldsymbol{A}\boldsymbol{Y}\boldsymbol{A}^{T}$. The branch current phasor $\boldsymbol{I}_{\mathrm{B}} = \boldsymbol{Y}\boldsymbol{A}^{T}\boldsymbol{V}_{\mathrm{N}}$. Thus the relationship between the branch current and the node injection current is

$$\boldsymbol{I}_{\mathrm{B}} = \boldsymbol{Y}\boldsymbol{A}^{T}\boldsymbol{Y}_{\mathrm{N}}^{-1}\boldsymbol{I}_{\mathrm{N}} \tag{2}$$

Mark the coefficient matrix $\boldsymbol{Y}\boldsymbol{A}^{T}\boldsymbol{Y}_{\mathrm{N}}^{-1}$ as $\boldsymbol{C}(\lambda)$, so that (2) can be simplified as

$$\boldsymbol{I}_{\mathrm{B}} = \boldsymbol{C}(\lambda)\boldsymbol{I}_{\mathrm{N}} \tag{3}$$

where $\boldsymbol{C}(\lambda)$ is a $b*n$ matrix, $b$ is the number of branches and $n$ is the number of nodes. The $k$th row in $\boldsymbol{C}(\lambda)$ represents the linear relationship between the $k$th branch current and the node injection currents, as shown in (4).

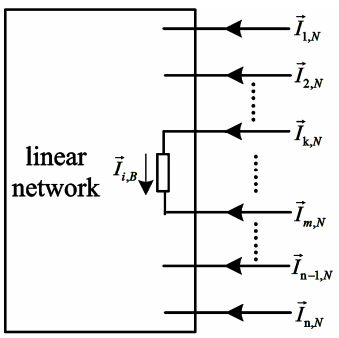


**Fig. 1.** Linear equivalent network of node injection current

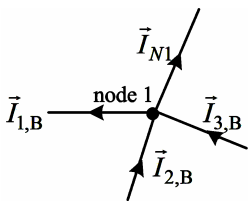


**Fig. 2.** Current flow graph of branches connected to node 1

$$\vec{I}_{k,\mathrm{B}} = \lambda_{k1}\vec{I}_{1,\mathrm{N}} + \lambda_{k2}\vec{I}_{2,\mathrm{N}} + \cdots + \lambda_{kn}\vec{I}_{n,\mathrm{N}} \tag{4}$$

The nodes in the network should observe Kirchhoff's current law. As shown in Fig. 2, node 1 is a load node and three branches are connected to node 1. According to the proportional distribution principle [14], the currents in Fig.2 have the following relationships

$$\begin{cases} \dfrac{\vec{I}_{2,\mathrm{B}}}{\vec{I}_{2,\mathrm{B}} + \vec{I}_{3,\mathrm{B}}}\vec{I}_{\mathrm{N1}} = \dfrac{\vec{I}_{\mathrm{N1}}}{\vec{I}_{\mathrm{N1}} + \vec{I}_{1,\mathrm{B}}}\vec{I}_{2,\mathrm{B}} \\ \dfrac{\vec{I}_{3,\mathrm{B}}}{\vec{I}_{2,\mathrm{B}} + \vec{I}_{3,\mathrm{B}}}\vec{I}_{\mathrm{N1}} = \dfrac{\vec{I}_{\mathrm{N1}}}{\vec{I}_{\mathrm{N1}} + \vec{I}_{1,\mathrm{B}}}\vec{I}_{3,\mathrm{B}} \end{cases} \tag{5}$$

Add up the two equations in (5), so that

$$\vec{I}_{\mathrm{N1}} = \frac{\vec{I}_{\mathrm{N1}}}{\vec{I}_{\mathrm{N1}} + \vec{I}_{1,\mathrm{B}}}\left(\vec{I}_{2,\mathrm{B}} + \vec{I}_{3,\mathrm{B}}\right) \tag{6}$$

Apply (3) to (6) and let $k = \dfrac{\vec{I}_{\mathrm{N1}}}{\vec{I}_{\mathrm{N1}} + \vec{I}_{1,\mathrm{B}}}$, thus the relationship between the load node current and the node injection currents can be gained:

$$\vec{I}_{\mathrm{N1}} = k\left(\boldsymbol{C}(\lambda_{2i})\boldsymbol{I}_{N} + \boldsymbol{C}(\lambda_{3i})\boldsymbol{I}_{N}\right) \tag{7}$$

Eq. (7) represents the relationship between the injection current of node 1 and the other node injection currents in the system. To generalize, Eq. (7) could be applied to other nodes to describe the relationship between the injection current of a certain node and the other node injection currents in the system. First, two line direction matrices $\boldsymbol{B}$ and $\boldsymbol{N}$ are defined. The positive direction matrix $\boldsymbol{B}$ is an $n*b$ matrix, and its element $\boldsymbol{B}_{ij}$ characterizes if the $j$th branch current is in the same direction as the injection current of node $i$. If yes, then $\boldsymbol{B}_{ij}$ is 1; otherwise, $\boldsymbol{B}_{ij}$ is 0. The negative direction matrix $\boldsymbol{N}$ is also an $n*b$ matrix, and its element $\boldsymbol{N}_{ij}$ characterizes if the $j$th branch current is in the opposite direction to the injection current of node $i$. If yes, then $\boldsymbol{N}_{ij}$ is 1; otherwise, $\boldsymbol{N}_{ij}$ is 0. Thus

$$\boldsymbol{I}_{N} = \boldsymbol{K}.*\boldsymbol{N}\boldsymbol{C}(\lambda)\boldsymbol{I}_{N} \tag{8}$$

where $\boldsymbol{K}$ is an $n*1$ matrix, and its element could be calculated as follows:

$$k_i = \frac{\vec{I}_{\mathrm{N}i}}{\vec{I}_{\mathrm{N}i} + B_i * \vec{I}_{\mathrm{B}}} = \frac{\vec{I}_{\mathrm{N}i}}{\vec{I}_{\mathrm{N}i} + B_i * \boldsymbol{C}\boldsymbol{I}_{N}} \tag{9}$$

Therefore, the expression of matrix $\boldsymbol{K}$ could be gained:

$$\boldsymbol{K} = \boldsymbol{I}_{N}./(\boldsymbol{I}_{N} + \boldsymbol{B}*\boldsymbol{C}\boldsymbol{I}_{N}) = 1./(1+\boldsymbol{B}\boldsymbol{C}) \tag{10}$$

Mark the coefficient matrix $\boldsymbol{K}.*\boldsymbol{NC}(\lambda)$ as $\boldsymbol{D}(\lambda)$ in (8), which is an *n*n* matrix, so that (10) can be put as:

$$\boldsymbol{I}_{\mathrm{N}} = \boldsymbol{D}(\lambda)\boldsymbol{I}_{\mathrm{N}} \tag{11}$$

When the system topology is given, the relationship between the line transmission power and the generator power and load power can be acquired. Besides, there exists certain corresponding relationship between the generator power and the load power. By searching for the generators and loads that are closely related with the overloaded line, fast and effective emergency load shedding strategy could be formed.

Transform the current expressions in (3) and (11) into active power expressions. On the phasor plane (where d-axis is the real axis and q-axis is the virtual axis), there exists the following relationship between power and current:

$$\begin{cases} P = U_d I_d + U_q I_q \\ Q = U_q I_d - U_d I_q \end{cases} \tag{12}$$

Then the branch injection power $P_{\mathrm{B}}$ can be expressed as:

$$P_{\mathrm{B}} = U_d I_{\mathrm{B}d} + U_q I_{\mathrm{B}q} \tag{13}$$

Take (3) for example. Transform (3) to the phasor plane, so that

$$\begin{cases} I_{\mathrm{B}d} = C_d I_{\mathrm{N}d} - C_q I_{\mathrm{N}q} \\ I_{\mathrm{B}q} = C_q I_{\mathrm{N}d} + C_d I_{\mathrm{N}q} \end{cases} \tag{14}$$

Apply (14) to (13), so that

$$\begin{aligned} P_{\mathrm{B}} &= C_d (U_d I_{\mathrm{N}d} + U_q I_{\mathrm{N}q}) + C_q (U_q I_{\mathrm{N}d} - U_d I_{\mathrm{N}q}) \\ &= C_d P_{\mathrm{N}} + C_q Q_{\mathrm{N}} \end{aligned} \tag{15}$$

In real power grid, line reactance is much bigger than line resistance. Therefore, for the elements in coefficient matrices $\boldsymbol{C}(\lambda)$ and $\boldsymbol{D}(\lambda)$, the real parts ($\boldsymbol{C}_d$ and $\boldsymbol{D}_d$) are much bigger than the virtual parts ($\boldsymbol{C}_q$ and $\boldsymbol{D}_q$). Thus, reactive power $Q_N$ is negligible and (15) can be further simplified as:

$$\boldsymbol{P}_{\mathrm{B}} = \boldsymbol{C}_d \boldsymbol{P}_{\mathrm{N}} \tag{16}$$

where $\boldsymbol{C}(\lambda)$ is the source-load branch synergy coefficient, which characterizes the relationship between the line transmission power and the generator power and load power.

Similarly, (11) can be transformed to the power expression:

$$\boldsymbol{P}_{\mathrm{N}} = \boldsymbol{D}_d \boldsymbol{P}_{\mathrm{N}} \tag{17}$$

where $\boldsymbol{D}(\lambda)$ is the source-load distribution synergy coefficient, which characterizes the relationship between the generator power and the load power. The calculation of $\boldsymbol{C}(\lambda)$ and $\boldsymbol{D}(\lambda)$ will not be affected by the change of power factor. Therefore, the following analysis is related to the network topology, and will not be affected by the change of power factor.

## 3. Line Overload Emergency Control Strategy Based on the Source-Load Synergy Coefficient

### 3.1 Generator tripping and load shedding emergency control

To apply the generator tripping and load shedding emergency control strategy, the generator and load control nodes need to be determined, as well as the control quantity of each control node. In traditional methods, the control quantity of a certain control node is determined according to the coefficient that characterizes the load shedding capability of the generator or load control node, in a successive or proportional way. The core idea of these methods is to minimize the total control quantity $\sum\Delta\boldsymbol{P}_{\mathrm{N}}$, i.e. to minimize the generator power output loss and the load loss, while realizing loading shedding for the overloaded line. However, it is neither rigorous nor realistic to equate the unit power loss of generator with that of load. For loads such as Medical and health, Government, etc., the economic loss caused by power outage is much bigger than that of Industrial and Commercial loads. Therefore, the control nodes and the corresponding control quantity cannot be determined merely according to the loading shedding capability of the nodes. Besides, due to the difference in generation characteristics, the per unit time coal consumption, pollutant discharge (mainly $SO_2$) and feed-in tariff of different generators are different. And the economic loss caused by the same power output reduction also differs. Thus, it is more realistic and rigorous to determine the control nodes and the control quantity of each control node by taking the economic loss factor into account.

According to (16), the control quantity matrix $\Delta\boldsymbol{P}_{\boldsymbol{N}}$ is related to the control quantity of the overloaded line $\Delta\boldsymbol{P}_{\boldsymbol{B}}$ in the following way:

$$\Delta\boldsymbol{P}_{\mathrm{B}} = \boldsymbol{C}_d \Delta\boldsymbol{P}_{\mathrm{N}} \tag{18}$$

where matrix $\boldsymbol{C}_d$ represents the load shedding capability of each control node to the overloaded line.

For different types of power customers (loads), the power outage loss functions are different. Shown in Table 1 is a statistical list of the power outage loss functions in a medium-sized city in China.

For different coal-fired generators, the per unit time feed-in tariff, coal consumption and pollutant discharge

**Table 1.** Power outage loss functions of different types of customers

| Customer type | Outage loss/yuan · KW$^{-1}$ | | | | | |
|---|---|---|---|---|---|---|
| | 1min | 30min | 1h | 2h | 4h | 8h |
| Industrial | 0.97 | 4.81 | 10.67 | 22.00 | 31.43 | 59.72 |
| Commercial | 3.93 | 16.50 | 37.33 | 75.00 | 312.97 | 637.42 |
| Medical & health | 45.50 | 75.60 | 159.98 | 431.93 | 826.37 | 1300.75 |
| Government | 0.00 | 40.50 | 85.32 | 141.41 | 246.29 | 434.16 |
| Public service | 0.00 | 20.15 | 42.66 | 98.12 | 166.84 | 275.22 |

functions can be expressed in (19)-(21) respectively [15].

$$F_{\mathrm{PG}i} = f_{\mathrm{PG}i} P_{\mathrm{G}i} \tag{19}$$

$$C_{\mathrm{RG}i} = a_{\mathrm{CR}i} P_{\mathrm{G}i}^2 + b_{\mathrm{CR}i} P_{\mathrm{G}i} + c_{\mathrm{CR}i} \tag{20}$$

$$P_{\mathrm{EG}i} = a_{\mathrm{PE}i} P_{\mathrm{G}i}^2 + b_{\mathrm{PE}i} P_{\mathrm{G}i} + c_{\mathrm{PE}i} \tag{21}$$

where $f_{\mathrm{PG}i}$ (yuan/MW.h) is the feed-in tariff coefficient of the $i$th generator. $a_{\mathrm{Cr}i}$ (t/MW$^2$h), $b_{\mathrm{Cr}i}$ (t/MW · h), and $c_{\mathrm{Cr}i}$ (t/h) are the coefficients of the coal consumption characteristics quadratic function. $a_{\mathrm{PE}i}$ (t/MW$^2$h), $b_{\mathrm{PE}i}$ (t/MW · h), and $c_{\mathrm{PE}i}$ (t/h) are the coefficients of the pollutant discharge characteristics quadratic function. $P_{\mathrm{Gi}}$ (MW) is the active power output of the $i$th generator.

Consider the generation characteristics of different generators and the power outage loss functions of different loads, and with a minimum system economic loss as the objective, the control quantity of each control node can be determined through optimization search. The overall economic loss of the system is:

$$F = F_A + F_B - F_C - F_D \tag{22}$$

$$\begin{cases} F_A = \sum_{i\in G} \Delta P_{\mathrm{G}i} * \left(f_{AP} - f_{\mathrm{P}i}\right) \\ F_B = \sum_{i\in L} \Delta P_{\mathrm{L}i} * f_{\mathrm{L}i} \\ F_C = k_C * \sum_{i\in G} \left( a_{\mathrm{CR}i} \left( P_{\mathrm{G}i}^2 - \left(P_{\mathrm{G}i} - \Delta P_{\mathrm{G}i}\right)^2 \right) + b_{\mathrm{CR}i} \left( P_{\mathrm{G}i} - \left(P_{\mathrm{G}i} - \Delta P_{\mathrm{G}i}\right)\right)\right) \\ F_D = k_D * \sum_{i\in G} \left( a_{\mathrm{PE}i} \left( P_{\mathrm{G}i}^2 - \left(P_{\mathrm{G}i} - \Delta P_{\mathrm{G}i}\right)^2 \right) + b_{\mathrm{PE}i} \left( P_{\mathrm{G}i} - \left(P_{\mathrm{G}i} - \Delta P_{\mathrm{G}i}\right)\right)\right) \end{cases} \tag{23}$$

where $F$ (yuan) is the overall cost, which consists of four parts. $F_A$ represents the power sale loss caused by reduction in generator power output, which is calculated by summing up the product of each regulating generator power variation and the generation profit (the power sale price $f_{AP}$ minus the feed-in tariff $f_{\mathrm{P}i}$). $F_B$ represents the total power outage loss of the loads. $F_C$ represents the saved coal consumption cost due to reduction in generator power output, which is the product of the coal price and the saved coal volume after the power output regulation. $F_D$ represents the saved pollutant discharge cost due to reduction in generator power output, which is the product of the pollutant discharge price and the reduced pollutant emission volume after the power output regulation.

Apart from the objective function being the minimum, other constraints should be considered. For example, it should be guaranteed that the system would not become unstable due to the emergency control.

First, according to the network power balance principle, the tripped generator power should equal to the shedded load power, i.e.

$$\sum_{i\in G} \left|\Delta P_{\mathrm{P}i}\right| = \sum_{j\in L} \left|\Delta P_{\mathrm{L}j}\right| \tag{24}$$

After the generator tripping and load shedding control, on the one hand, the overflowing load on the overloaded line should be eliminated, and the load shedding amount of the overloaded line is

$$\Delta P_{\mathrm{B}i} = (1-\alpha) P_{\mathrm{B}i\max} - P_{\mathrm{B}i} \tag{25}$$

where $P_{\mathrm{B}i}$ is the line transmission power before the generator tripping and load shedding control. $\alpha$ is the line thermal stability margin and $P_{\mathrm{B}i\max}$ is the maximum line transmission power.

Substitute the line power on the left side of (25) with the node injection power, so that

$$\boldsymbol{C}_{di} \Delta \boldsymbol{P}_N = (1-\alpha) P_{\mathrm{B}i\max} - P_{\mathrm{B}i} \tag{26}$$

On the other hand, the other lines in the system should not be overloaded after the emergency control. Therefore, the following condition needs to be satisfied:

$$\boldsymbol{P}_{\mathrm{B}} + \boldsymbol{C}_d \Delta \boldsymbol{P}_N \le (1-\alpha) \boldsymbol{P}_{\mathrm{B}\max} \tag{27}$$

Besides, the generator power inequality constraint and the node voltage inequality constraint should be considered:

$$P_{\mathrm{G}i\min} \le P_{\mathrm{G}i} \le P_{\mathrm{G}i\max} \tag{28}$$

$$V_{\mathrm{N}i\min} \le V_{\mathrm{N}i} \le V_{\mathrm{N}i\max} \tag{29}$$

After the emergency control, the system should be able to maintain transient stability, i.e. the energy function and the power angle should both remain within limit:

$$V_c < V_{cr} \tag{30}$$

$$\delta_{\max} < \delta_r \tag{31}$$

where $V_{cr}$ is the transient energy function stability limit, $\delta_{\max}$ is the maximum power angle difference in the system, and$\delta_{\mathrm{r}}$ is the power angle stability limit.

Based on the above factors, the generator tripping and load shedding emergency control model could be established:

$$s.t.\quad \begin{cases} \min F = F_A + F_B - F_C - F_D \\ \sum_{i\in G}\left|\Delta P_{\mathrm{P}i}\right| = \sum_{j\in L}\left|\Delta P_{\mathrm{L}j}\right| \\ \boldsymbol{C}_{di}\Delta \boldsymbol{P}_N = (1-\alpha)P_{\mathrm{B}i\max} - P_{\mathrm{B}i} \\ \boldsymbol{P}_{\mathrm{B}} + \boldsymbol{C}_d\Delta \boldsymbol{P}_N \le (1-\alpha)\boldsymbol{P}_{\mathrm{B}\max} \\ P_{\mathrm{G}i\min} \le P_{\mathrm{G}i} \le P_{\mathrm{G}i\max} \\ V_{\mathrm{N}i\min} \le V_{\mathrm{N}i} \le V_{\mathrm{N}i\max} \\ V_c < V_{cr} \\ \delta_{\max} < \delta_r \end{cases} \tag{32}$$

where $\boldsymbol{G}$ is the generator control nodes set. If reducing the injection power of a certain generator node could reduce the power on the overloaded line, then this generator node is added to $\boldsymbol{G}$, i.e. generator nodes with $\boldsymbol{C}_{di}>0$ are selected. $\boldsymbol{L}$ is the load control nodes set. If reducing the injection power of a certain load node could reduce the power on the overloaded line, then this load node is added to $\boldsymbol{L}$. Since the injection power of the load node is in the reverse direction, load nodes with $\boldsymbol{C}_{di}<0$ are selected. The control quantity of each control node is determined with the optimization algorithm according to the objective function and the constraints.

The DFPSO is used for optimization search. Mark the objective functions that are related with the active power regulation $\Delta\boldsymbol{P}_{\mathrm{N}}$ as fitness function $f(\Delta P_1, \Delta P_2,..., \Delta P_{\mathrm{n}})$, and the constraints related with $\Delta\boldsymbol{P}_{\mathrm{N}}$ are marked as fitness function $v(\Delta P_1, \Delta P_2,..., \Delta P_{\mathrm{n}})$. According to (32), the optimization function is:

$$\begin{cases} \min f(\Delta P_1, \Delta P_2, ..., \Delta P_n) = F_A + F_B - F_C - F_D \\ v(\Delta P_1, \Delta P_2, ..., \Delta P_n) = \sum_{j=1}^{q}\max\left(0, P_{\mathrm{B}j} + C_{dj}\Delta \boldsymbol{P}_N - (1-\alpha)P_{\mathrm{B}j\max}\right) + \\ \qquad \left|\sum_{i\in G}\Delta P_{\mathrm{P}i} - \sum_{j\in L}\Delta P_{\mathrm{L}j}\right| + \left|\boldsymbol{C}_{di}\Delta \boldsymbol{P}_N - (1-\alpha)P_{\mathrm{B}i\max} + P_{\mathrm{B}i}\right| \end{cases} \tag{33}$$

### 3.2 Load power restoration control

After the generator tripping and load shedding control, the line overload problem is effectively solved. However, this is at the cost of much load loss. In order to guarantee a continuous and reliable power supply, some of the untripped generators could be selected to provide power supply to some of the shedded load, so that load loss could be reduced. The purpose of load power restoration is to maximize the economic benefits, and its objective function takes the same form as that in the generator tripping and load shedding control, only that the optimization search is for the maximum value of the objective function. Meanwhile, the constraints are different. The equality constraint in (25) is deleted and an inequality constraint is added, which is about the load power restoration upper limit, i.e. the power restored to each load node should not exceed the previously shedded load:

$$\Delta P'_{\mathrm{L}i} \le \Delta P_{\mathrm{L}i} \tag{34}$$

Based on the above analysis, the mathematical model of load power restoration could be established:

$$s.t.\quad \begin{cases} \max F = F_A + F_B - F_C - F_D \\ \sum_{i\in G}|\Delta P_{\mathrm{P}i}| = \sum_{j\in L}|\Delta P_{\mathrm{L}j}| \\ \Delta P'_{\mathrm{L}i} \le \Delta P_{\mathrm{L}i} \\ \boldsymbol{P}_{\mathrm{B}} + \boldsymbol{C}_d\Delta \boldsymbol{P}_N \le (1-\alpha)\boldsymbol{P}_{\mathrm{B}\max} \\ P_{\mathrm{G}i\min} \le P_{\mathrm{G}i} \le P_{\mathrm{G}i\max} \\ V_{\mathrm{N}i\min} \le V_{\mathrm{N}i} \le V_{\mathrm{N}i\max} \\ V_c < V_{cr} \\ \delta_{\max} < \delta_r \end{cases} \tag{35}$$

where $\boldsymbol{L}$ is the set of load nodes to which power supply is to be restored, and it consists of all the load nodes that participated in the load shedding control. $\boldsymbol{G}$ is the set of generator nodes which are to restore power supply to the load nodes in $\boldsymbol{L}$. The generator nodes corresponding to the elements in $\boldsymbol{L}$ with $\boldsymbol{D}_d(\lambda)>0$ are selected, excluding the generators nodes that participated in the generator tripping control. Similarly, the control quantity of each generator node is determined with the optimization algorithm according to the objective function and the constraints.

Similarly, the DFPSO is used for optimization search. According to (35), the objective function fitness function $f(\Delta P_1, \Delta P_2,..., \Delta P_{\mathrm{n}})$ and the constraints fitness function $v(\Delta P_1, \Delta P_2,..., \Delta P_{\mathrm{n}})$ are as follows:

$$\begin{cases} \max f(\Delta P_1, \Delta P_2, ..., \Delta P_n) = F_A + F_B - F_C - F_D \\ v(\Delta P_1, \Delta P_2, ..., \Delta P_n) = \sum_{j=1}^{q}\max\left(0, P_{\mathrm{B}j} + C_{dj}\Delta \boldsymbol{P}_N - (1-\alpha)P_{\mathrm{B}j\max}\right) + \\ \qquad \left|\sum_{i\in G}\Delta P_{\mathrm{P}i} - \sum_{j\in L}\Delta P_{\mathrm{L}j}\right| + \sum_{j=1}^{m}\max\left(0, P'_{Lj} - P_{Lj}\right) \end{cases} \tag{36}$$

Add up the two calculation results, so that the final regulation control quantity could be gained: $\Delta\boldsymbol{P}_{\mathrm{Nf}} = \Delta\boldsymbol{P}_{\mathrm{N1}} + \Delta\boldsymbol{P}_{\mathrm{N2}}$.

## 4. Simulation Verification

The IEEE 10-machine 39-bus system (rated frequency 60Hz) [16] is used to verify the correctness and

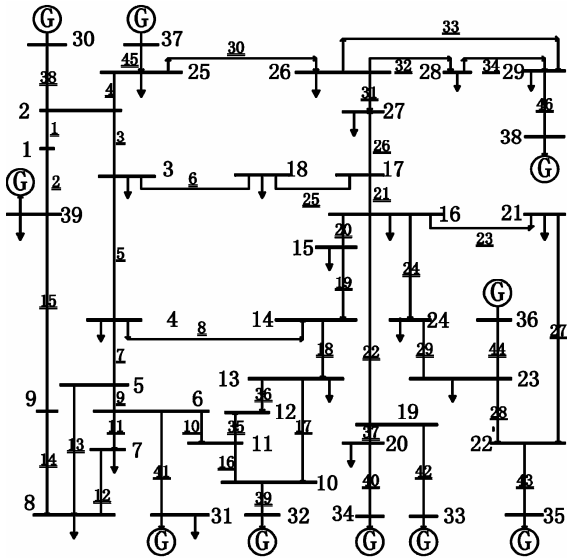

**Fig. 3.** IEEE 10-machine 39-bus system

effectiveness of the proposed method. As shown in Fig. 3, line 29 and line 27 are the trunk lines through which generator 35 and 36 transmit power to other nodes. Suppose fault occurs on line 29 and it is cut off after the fault, then the pre-fault transmission power on line 29 will be transferred, which will cause line 27 to be overloaded. If the transmission power on line 27 exceeds the transmission power limit, generator tripping and load shedding control will be needed for load shedding of the overloaded line, as well as load power restoration measures to minimize the economic loss.

### 4.1 Source-load synergy coefficient

After line 29 is cut off, the network topology will change, thus the original incidence matrix A and branch admittance matrix Y need to be modified first, by deleting the elements in the two matrices that correspond to line 29. According to (2) and (8), the system source-load branch synergy coefficient Cd(λ) and source-load distribution synergy coefficient Dd(λ) after line 29 is cut off can be calculated. The source-load branch synergy coefficient of line 27 is shown in Table 2.

**Table 2.** Source-load branch synergy coefficient of line 27

| Node | $C_{d27}$ | Node | $C_{d27}$ | Node | $C_{d27}$ | Node | $C_{d27}$ |
|---|---|---|---|---|---|---|---|
| 1 | -0.0348 | 11 | -0.0323 | 21 | -0.0246 | 31 | -0.0326 |
| 2 | -0.0332 | 12 | -0.0322 | 22 | 0.9797 | 32 | -0.0323 |
| 3 | -0.0322 | 13 | -0.0321 | 23 | 0.9805 | 33 | -0.0288 |
| 4 | -0.0322 | 14 | -0.0317 | 24 | -0.0287 | 34 | -0.0288 |
| 5 | -0.0327 | 15 | -0.0297 | 25 | -0.0333 | 35 | 0.9797 |
| 6 | -0.0326 | 16 | -0.0287 | 26 | -0.0332 | 36 | 0.9805 |
| 7 | -0.0329 | 17 | -0.0304 | 27 | -0.0320 | 37 | -0.0333 |
| 8 | -0.0330 | 18 | -0.0311 | 28 | -0.0343 | 38 | -0.0343 |
| 9 | -0.0347 | 19 | -0.0288 | 29 | -0.0343 | 39 | -0.0352 |
| 10 | -0.0322 | 20 | -0.0288 | 30 | -0.0333 | – | – |

Note: '—' represents no relevant node or parameter.

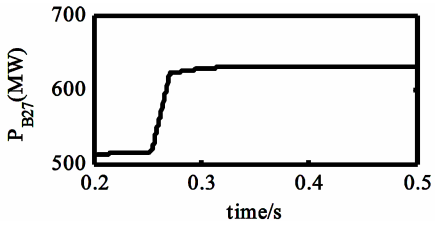


**Fig. 4.** Transmission power variation in the case of line 27 overload

**Table 3.** Feed-in tariff and active power limit of generators

| Generator | Feed-in tariff $f_{Pi}$ (yuan/kwh) | Generator active power limit (MW) | |
|---|---|---|---|
| | | Upper limit | Lower limit |
| 30 | 0.22 | 600 | 200 |
| 31 | 0.56 | 600 | 200 |
| 32 | 0.32 | 800 | 300 |
| 33 | 0.31 | 800 | 300 |
| 34 | 0.56 | 600 | 200 |
| 35 | 0.26 | 600 | 200 |
| 36 | 0.28 | 600 | 200 |
| 37 | 0.62 | 600 | 200 |
| 38 | 0.68 | 1000 | 400 |
| 39 | 0.78 | 300 | 100 |

**Table 4.** Coal consumption characteristics of generators

| Generator | Coal consumption coefficients | | |
|---|---|---|---|
| | $a_{CRi}$ (t/MW$^2$h) | $b_{CRi}$ (t/MW · h) | $c_{CRi}$(t/h) |
| 30 | 0.0041 | 0.22 | 7.33 |
| 31 | 0.0045 | 0.24 | 7.51 |
| 32 | 0.00337 | 0.181 | 5.53 |
| 33 | 0.00337 | 0.181 | 5.53 |
| 34 | 0.0044 | 0.23 | 7.57 |
| 35 | 0.0051 | 0.29 | 8.12 |
| 36 | 0.0051 | 0.29 | 8.12 |
| 37 | 0.0042 | 0.23 | 7.41 |
| 38 | 0.00315 | 0.168 | 5.25 |
| 39 | 0.00563 | 0.299 | 9.39 |

### 4.2 Generator tripping and load shedding control

Suppose a three-phase fault occurs on line 29 at t=0.25s, and after 50ms line 29 is cut off by the line primary protection. Due to power transfer, the power on line 27 increases to $P_{B27}$=630.12MW, which exceeds the transmission power limit ($P_{B27max}$=570MW). The transmission power on line 27 undergoes significant variation, as shown in Fig. 4.

In this case, generator tripping and load shedding control is needed for load shedding of line 27. According to engineering practice [17], some non-electrical parameters are put forward in Table 3 and Table 6. The feed-in tariff, coal consumption and pollutant discharge functions of the generators are shown in Table 3-Table 5. The power outage loss functions of the load nodes are shown in Table 6, where the unit time is 1h.

The generator nodes in Table 2 with $C_d(\lambda_{27})>0$ are selected for the generator tripping control, i.e. generator

**Table 5.** pollutant discharge characteristics of generators

| Generator | Pollutant discharge coefficients | | |
|---|---|---|---|
| | $a_{CRi}$ (t/MW$^2$h) | $b_{CRi}$ (t/MW · h) | $c_{CRi}$(t/h) |
| 30 | 0.01195 | 0.58 | 0.1763 |
| 31 | 0.01125 | 0.6 | 0.1877 |
| 32 | 0.00674 | 0.362 | 0.1106 |
| 33 | 0.00674 | 0.362 | 0.1106 |
| 34 | 0.0113 | 0.605 | 0.1823 |
| 35 | 0.0117 | 0.624 | 0.1953 |
| 36 | 0.0117 | 0.624 | 0.1953 |
| 37 | 0.01145 | 0.613 | 0.1906 |
| 38 | 0.0063 | 0.404 | 0.138 |
| 39 | 0.01576 | 0.837 | 0.2629 |

**Table 6.** Power outage loss functions of loads

| Load node | Outage loss function (yuan · KW$^{-1}$) | Load node | Outage loss function (yuan · KW$^{-1}$) |
|---|---|---|---|
| 3 | 10.67 | 21 | 85.32 |
| 4 | 37.33 | 23 | 37.33 |
| 7 | 37.33 | 24 | 10.67 |
| 8 | 85.32 | 25 | 37.33 |
| 12 | 159.98 | 26 | 10.67 |
| 15 | 10.67 | 27 | 42.66 |
| 16 | 37.33 | 28 | 10.67 |
| 18 | 10.67 | 29 | 42.66 |
| 20 | 10.67 | – | – |

Note: '—' represents no relevant node or parameter.

nodes 35 and 36 are selected as the control nodes, which constitute $G$. Similarly, the load nodes in Table 2 with $C_d(\lambda_{27})<0$ are selected for the load shedding control, i.e. load nodes 3, 4, 7, 8, 12, 15, 16, 18, 20, 21, 24, 25, 26, 27, 28 and 29 are selected as the control nodes, which constitute $\boldsymbol{L}$.

After the control nodes are selected, the objective function $f(\Delta P_1, \Delta P_2,..., \Delta P_n)=\min(F_A+F_B+F_C+F_D)$ can be determined, according to (22) and (23). Relevant coefficients of the generator control nodes set $\boldsymbol{G}$ and the load control nodes set $\boldsymbol{L}$ can be found in Table 2-Table 6.

The constraints can be determined according to (32). The line thermal stability margin $\alpha$=5%, and line transmission power limit $P_{B27max}$=570MW, thus the amount of load that needs to be shedded is $P_{B27}-(1-\alpha)P_{B27max}$ = 88.62MW. The constraints related with the node injection power form the constraints boundary fitness function $v(\Delta P_1, \Delta P_2,..., \Delta P_n)$ according to (33), and the DFPSO is used for optimization search. After the optimization search, the control quantity of each control node is shown in Table 7, which is marked as $\Delta \boldsymbol{P}_{N1}$. It can be seen from Table 7 that, generator nodes 35 and 36 both participate in the generator tripping control, and load nodes 26, 28, 29 also shed some load.

It can be seen from (16) that, the load shedding amount of line 27 is $\Delta \boldsymbol{P}_B = \boldsymbol{C}_d \Delta \boldsymbol{P}_{N1}$ = 88.64MW. Through information exchange between relay protection device and stability control device [15], the generator tripping and load shedding control is applied at $t$=0.5s. After the load shedding, the transmission power on line 27 is 541.48MW

**Table 7.** Generator tripping and load shedding control search result

| Node | Control quantity/MW | Node | Control quantity/M |
|---|---|---|---|
| 35 | -52.14 | 18 | 0 |
| 36 | -41.55 | 20 | 0 |
| 3 | 0 | 21 | 0 |
| 4 | 0 | 24 | 0 |
| 7 | 0 | 25 | 0 |
| 8 | 0 | 26 | -24.45 |
| 12 | 0 | 27 | 0 |
| 15 | 0 | 28 | -56.73 |
| 16 | 0 | 29 | -12.51 |

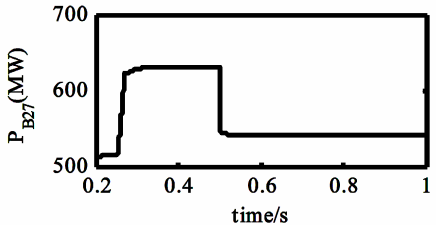


**Fig. 5.** Transmission power variation of line 27 after generator tripping and load shedding control

(see Fig. 5), which is less than $P_{B27max}$, and all the constraints are met. The minimum system per unit time economic loss caused by the generator tripping and load shedding control is $F_l$=1175606.7yuan/h. After the emergency control, the lowest bus voltage in the system (Bus 31) is 0.9816pu, and the lowest bus frequency (Bus 38) is 59.8985Hz. Thus the system could maintain its stability.

### 4.3 Load power restoration control

It can be seen from Table 7 that, some of the load at nodes 26, 28, 29 is shedded due to the emergency control. In order to improve the reliability of power supply and minimize the economic loss caused by power outage, power supply is restored to some of the shedded load by modestly increasing the power output of some generators. The upper limit of power restored to each load node is the shedded value in $\Delta \boldsymbol{P}_{N1}$.

Similarly, the control nodes are selected first. For load control nodes, the three nodes to which power supply is to be restored form the load nodes set $\boldsymbol{L}$. For generator control nodes, the untripped generators with $\boldsymbol{D}_d(\lambda)>0$ (i.e. the generators with a supply relationship with the load nodes to which power supply is to be restored) are selected. The source-load distribution synergy coefficients of load nodes 26, 28, 29 are shown in Table 8. According to the above search principle (i.e. the union of the search results of three load nodes), generator nodes 30, 37, 38 and 39 are selected as the control nodes, which form $\boldsymbol{G}$.

After the control nodes are selected, the objective function could be determined according to (23) and (25), i.e. $f(\Delta P_1, \Delta P_2,..., \Delta P_n)=\max(F_A+F_B+F_C+F_D)$. The

**Table 8.** Source-load distribution synergy coefficient of load 26, 28, 29

| Generator | $\boldsymbol{D}_d(\lambda_{26})$ | $\boldsymbol{D}_d(\lambda_{28})$ | $\boldsymbol{D}_d(\lambda_{29})$ |
|---|---|---|---|
| 30 | 0.1351 | -0.0144 | -0.0001 |
| 31 | -0.0276 | -0.0153 | -0.0001 |
| 32 | -0.0434 | -0.0152 | -0.0001 |
| 33 | -0.1780 | -0.0146 | -0.0001 |
| 34 | -0.1780 | -0.0146 | -0.0001 |
| 37 | 0.2080 | -0.0140 | -0.0001 |
| 38 | 0.3875 | 0.3388 | 0.5104 |
| 39 | 0.0667 | -0.0160 | -0.0001 |

**Table 9.** Load power restoration search result

| Node | Control quantity/MW | Node | Control quantity/M |
|---|---|---|---|
| 26 | 13.77 | 37 | 10.77 |
| 28 | 49.80 | 38 | 25.38 |
| 29 | 4.17 | 39 | 26.25 |
| 30 | 5.34 | – | – |

Note: '—' represents no relevant node or parameter

**Table 10.** Control quantity of the line overload emergency control strategy based on source-load synergy coefficient

| Node | Control quantity/M | Node | Control quantity/M |
|---|---|---|---|
| 3 | 0 | 30 | 5.34 |
| 4 | 0 | 31 | 0 |
| 7 | 0 | 32 | 0 |
| 8 | 0 | 33 | 0 |
| 12 | 0 | 34 | 0 |
| 15 | 0 | 35 | -52.14 |
| 16 | 0 | 36 | -41.55 |
| 18 | 0 | 37 | 10.77 |
| 20 | 0 | 38 | 25.38 |
| 21 | 0 | 39 | 26.25 |
| 23 | 0 | – | – |
| 24 | 0 | – | – |
| 25 | 0 | – | – |
| 26 | -10.68 | – | – |
| 27 | 0 | – | – |
| 28 | -6.93 | – | – |
| 29 | -8.34 | – | – |

Note: '—' represents no relevant node or parameter

parameters are the same as in the generator tripping and load shedding control, only that the maximum value of the objective function is pursued in the power restoration control, not the minimum value. The constraints could be determined according to (36), which then form the constraints boundary fitness function $v(\Delta P_1, \Delta P_2,..., \Delta P_n)$. Again, the DFPSO is used for optimization search. The control quantity of each control node is shown in Table 9, which is marked as $\Delta \boldsymbol{P}_{N2}$. Some of the shedded load at nodes 26, 28 and 29 are restored to power by increasing the power output of generator 30, 37, 38 and 39.

This search result meets all the equality and inequality constraints. The saved system per unit time economic loss is $F_2$=682638.0yuan/h. After the power restoration, the lowest bus voltage in the system (Bus 31) is 0.9811pu, and the lowest bus frequency (Bus 36) is 59.7058Hz. Thus the system could maintain its stability.

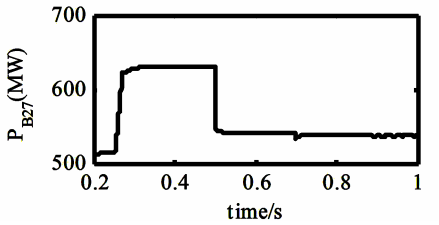


**Fig. 6.** Transmission power variation of line 27 after load power restoration

The overall control quantity of each node in the overload emergency control strategy is $\Delta \boldsymbol{P}_{Nf}=\Delta \boldsymbol{P}_{N1}+\Delta \boldsymbol{P}_{N2}$, which is shown in detail in Table 10.

After the load power restoration control is applied at t=0.7s, according to (16), the load shedding amount of line 27 is $\Delta \boldsymbol{P}_B = \boldsymbol{C}_d(\Delta \boldsymbol{P}_{N1} + \Delta \boldsymbol{P}_{N2}) = 93.27$ MW. The transmission power on line 27 becomes 536.85MW (see Fig. 6), which is less than $P_{B27max}$, and all the constraints are met. It can be seen from Fig. 6 that, power restoration to some of the shedded load improves the economic benefits, without causing re-overload in the original overloaded line. The minimum system per unit time economic loss caused by the whole emergency control is $F_1-F_2$= 492968.7yuan/h.

In the manuscript, generator tripping control and load shedding control and load power restoration control are applied. For generator tripping control and load shedding control, the optimization function is (33), and the selected nodes and control quantity are determined by $\boldsymbol{C}(\lambda)$. For load power restoration control, the optimization function is (36), and the selected nodes are determined by $\boldsymbol{D}(\lambda)$ as well as the control quantity is determined by $\boldsymbol{C}(\lambda)$. According to the analysis of Section Ⅱ, the calculation of $\boldsymbol{C}(\lambda)$ and $\boldsymbol{D}(\lambda)$ will not be affected by the change of power factor. Therefore, the analysis result in the manuscript is related to the network topology, and will not be affected by the change of power factor.

## 5. Conclusion

A line overload emergency control strategy based on the source-load synergy coefficient is proposed in this paper. On the premise that the overload is eliminated, a minimum system economic loss is also pursued. The whole control strategy consists of two parts: the generator tripping and load shedding control, and the load power restoration control. The first part is focused on fast load shedding of the overloaded line through generator tripping and load shedding control measures, so that the safety and stability of the system could be guaranteed. This part is the basis of the whole control strategy. The second part is focused on

the continuity and reliability of power supply. By increasing the power output of some of the untripped generators, power supply could be restored to some of the shedded loads. Thus the economic loss caused by load power outage could be minimized. This part is the extention of the emergency control. The proposed strategy has the following characteristics:

(1) Compared with control strategy based on sensitivity degree and control strategy based on traditional objective optimization, a number of constraints are put forward concerning safety and stability of the whole system. Thus, the proposed emergency control strategy is safe and reliable.

(2) The grid loss caused by the emergency control is evaluated from the viewpoint of the economic loss. By taking the generation characteristics of different generators and the economic loss characteristics of different loads into account, the proposed strategy is suitable for practical engineering.

## Acknowledgment

This work is supported by the National Key R&D Program of China (2016 YFB0900604), and the Chinese University Scientific Fund Project (2018JQ01).

## References

[1] Nedic D.P, Dobson, I, Kirschen, D.S, Carreras B.A, and Lynch, V.E, "Criticality in a cascading failure blackout model," *Int J Electr Power Energy Syst*, vol. 28, no. 9, pp. 627-633, Nov.2006.

[2] Halim Abu B.A., Yatim F.M, Yusof S, and Othman M.R, "Analysis of overload conditions in distance relay under severe system contingencies," *Int J Electr Power Energy Syst*, vol. 32, no. 2, pp. 345-350, Jun.2010.

[3] Qi J.J, Mei S.W, and Liu F, "Blackout model considering slow process," *IEEE Trans. Power Syst.*, vol. 28, no. 3, pp. 3274-3283, Aug.2013.

[4] Otomega, B., Marinakis, A., Glavic, M., and Van Cutsem, T, "Model predictive control to alleviate thermal overloads", *IEEE Trans. Power Syst.*, vol. 22, no. 3, pp. 1384-1385, Aug.2007.

[5] Abrantes H.D., and Castro C.A, "A new efficient nonlinear programming-based method for branch overload elimination," *Electr. Power Comp. Syst.*, vol. 30, no. 6, pp. 525-537, Jun.2002.

[6] Girgis, Adly A., and Mathure, Shruti, "Application of active power sensitivity to frequency and voltage variations on load shedding," *Electr Power Syst Res*, vol. 80, no. 6, pp. 306-310, Mar.2010.

[7] Ota H., Kitayama Y., Ito H., Fukushima N.,Omata K., Morita K., and Kokai Y., "Development of transient stability control system (TSC system) based on on-line stability calculation," *IEEE Trans. Power Syst.*, vol. 11, no. 3, pp. 1463-1472, Aug.1996.

[8] Xu H.M, Bi T.S, Huang S.F, Yang Q.X, and Ma R. "Study on wide area measurement system based control srategy to prevent cascading trips," *Proceedings of the CSEE*, vol. 27, no. 19, pp. 32-38, Jul.2007.

[9] Emmanouil M.V and Nikos D.H. "A particle swarm optimization method for power system dynamic security control," *IEEE Trans. Power Syst.*, vol. 25, no. 2, pp. 1032-1041, May.2010.

[10] Liu K, Dong X, Wang B, Shi S. "Impact Analysis of Fault Dynamic Process on Power Flow Identification," *Automation of Electric Power Systems*, vol. 28, no. 22, pp. 32-36, July.2011.

[11] Wu P, Cheng H, Qu G. "Algorithm to Solve Interval Minimum Load Cutting Problem for Transmission Planning," *Proceedings of the CSEE*, vol. 32, no. 28, pp. 41-146, Aug.2013.

[12] J. Kennedy and R. Eberhart, "Particle swarm optimization," *in Proc. 1995 IEEE Int. Conf. Neural Networks*, vol. 4, pp. 1942-1948.

[13] Zhang T, Yu J, Yang X.Y, and Liao B. "Improved particle swarm optimization algorithm for cloud computing task scheduling," *Computer Engineering and Applications*, vol. 49, no. 19, pp. 68-72, 2013.

[14] Dai Y., Liu X.D., Ni Y.X., Wen F.S., Han Z.X., Shen C.M., Wu Felix F., "A cost allocation method for reactive power service based on power flow tracing," *Electr Power Syst Res*, vol. 64, no. 1, pp. 59-65, Jan.2006.

[15] Xu S.L, Yu J.L. "Composite flow state computation of power network based on electrical dissection information," *Power System Technology*, vol. 37, no. 2, pp. 425-430, Feb.2013.

[16] Ma J, Li J.L, James S.T, Andrew J.A, Yang Q.X, and A. G. Phadke. "A fault steady state component-based wide area backup protection algorithm," *IEEE Trans. Smart Grid*, vol. 2, no. 3, pp. 468-475, Sep.2011.

[17] Zhou Z, Wang X, Du D, Li Y, Li M. "A Coordination Strategy Between Relay Protection and Stability Control Under Overload Conditions," *Proceedings of the CSEE*, vol. 32, no. 28, pp. 146-153, Oct.2013.

**Jing Ma** He was born in Hebei Province, China on February 25, 1981. He received his B.S. and Ph.D. degree from North China Electric Power University, China, in 2003 and 2008, respectively. He has been a visiting research scholar in the Bradley Department of Electrical and Computer Engineering, Virginia Polytechnic Institute and State University from 2008 to 2009. He is currently a professor

in the School of Electrical and Electronic Engineering, North China Electric Power University, China. His major interests include power system equipment modeling and protection.

**Wenbo Kang** He was born in Jilin Province, China on January 28, 1994. He is currently a Master student in the School of Electrical and Electronic Engineering, North China Electric Power University, China. He received his B.S. degree from North China Electric Power University in 2016. His interests mainly include power system protection and control.

**James S. Thorp** He is the Hugh P. and Ethel C. Kelley Professor of Electrical and Computer Engineering and Department Head of the Bradley Department of Electrical and Computer Engineering at Virginia Tech. He was the Charles N. Mellowes Professor in Engineering at Cornell University from 1994-2004. He was the Director of the Cornell School of Electrical and Computer Engineering from 1994 to 2001, a Faculty Intern, American Electric Power Service Corporation in 1976-77 and an Overseas Fellow, Churchill College, Cambridge University in 1988. He was an Alfred P. Sloan Foundation National Scholar and was elected a Fellow of the IEEE in 1989 and a Member of the National Academy of Engineering in 1996. He received the 2001 Power Engineering Society Career Service award, the 2006 IEEE Outstanding Power Engineering Educator Award, and shared the 2007 Benjamin Franklin Medal with A.G. Phadke.